Factors Controlling the ^{17}O NMR Chemical Shift in Ionic Mixed Metal Oxides

Timothy J. Bastow,† Peter J. Dirken,‡ and Mark E. Smith*,†,‡

CSIRO Division of Materials Science and Technology, Private Bag 33, Rosebank MDC, Clayton, Victoria 3169, Australia, and Physics Department, University of Kent, Canterbury, Kent, CT2 7NR, U.K.

Harold J. Whitfield

Department of Applied Physics, Royal Melbourne Institute of Technology, P.O. Box 2476W, Melbourne, Victoria 3001, Australia

Received: July 25, 1996[⊗]

A wide range of ^{17}O-enriched phases ABO_3 and A_2BO_3 (A = Li, Na, Ca, Sr, Ba, and La; B = Ti, Zr, Sn, Nb, and Al) and related compounds has been synthesized and studied using ^{17}O magic angle spinning (MAS) NMR spectroscopy. In these highly ionic phases, the ^{17}O electric field gradients are small, and as a result highly resolved NMR spectra that reveal subtle structural inequivalences are observed. For titanates and zirconates the ^{17}O chemical shifts fall in distinct, well-defined regions (372−564 and 280−376 ppm, respectively). The ratio of isotropic ^{17}O chemical shifts from isostructural titanates and zirconates with the same A cation is constant, and this ratio is close to the ratio of the polarizing powers of titanium and zirconium. The B cation appears to be the dominant influence in determining the ^{17}O chemical shift in these compounds. Additionally the number of oxygen resonances and the shift difference between them increases as the symmetry of the structure decreases. ^{119}Sn MAS NMR has been applied to a variety of stannates and shows a large shift difference (68.2 ppm) between $CaSnO_3$ phases with the ilmenite and $GdFeO_3$ perovskite type crystal structures. ^{27}Al and ^{17}O MAS NMR have been used to study the conversion of lanthanum and aluminum sol−gel precursors to crystalline $LaAlO_3$ perovskite. ^{17}O NMR proves to be more informative than ^{27}Al NMR and shows that the formation of $LaAlO_3$ proceeds via the reaction of separate lanthanum and aluminum oxides initially formed.

Introduction

The perovskite structure ABO_3 is one of the most important in materials science and geophysics occurring widely in ferroelectrics, piezoelectrics, thin film electronics, and optical devices.[1] An estimated 80 vol % of the Earth's lower mantle is thought to be composed of $(Mg,Fe)SiO_3$ perovskite, making it the most abundant mineral in the Earth's mantle,[2] so that interpretation of seismic data relies heavily on knowledge of the perovskite crystal structure. The ideal perovskite structure (e.g., $SrTiO_3$) has cubic symmetry (*Pm*3*m*) with the only variable the unit-cell parameter *a*, and consists of corner-linked octahedra of oxygen anions with B cations at their centers. The A cations fill the cuboctahedral interstices between the octahedra with 12 coordination.[3,4] Noncubic perovskite structures are subsequently formed by either cationic displacement (e.g., $BaTiO_3$), tilting of the octahedra (e.g., the mineral perovskite, $CaTiO_3$), or a combination of both (e.g., $NaNbO_3$).[4] To a first approximation the deviation from cubic symmetry is controlled by the relative sizes of the ions within the lattice. This is described by the tolerance factor $t = (R_A + R_B)/(R_B + R_O)$, with $t = 1$ in the case of an ideal framework structure.[3] Departures of t from unity result in a loss of cubic symmetry and eventually, if t varies significantly, the adoption of another structure type altogether. For instance, in the case of $B = Ti^{4+}$, $SrTiO_3$ ($r_{Sr^{2+}} = 1.37$ Å, $t = 0.97$) has cubic symmetry, $CaTiO_3$ ($r_{Ca^{2+}} = 1.16$ Å, $t = 0.89$) has orthorhombic symmetry, and the Li_2TiO_3 structure ($r_{Li^+} = 0.68$ Å, $t = 0.67$) is monoclinic.[4] The latter structure is not a perovskite structure, but is closely related to it. For $t > 1$, $BaTiO_3$ ($r_{Ba^{2+}} = 1.52$ Å, $t = 1.02$) the symmetry is tetragonal.[3] In a cubic system all the oxygens are equivalent, but as the symmetry is lowered the number of inequivalent oxygen sites increases to a maximum of three. Deviations of the perovskite structure from cubic to lower symmetry and the associated loss of a center of symmetry are critical because they are directly linked to many of the technologically important properties of these materials. For example, $BaTiO_3$ is a widely used ferroelectric whose electric dipole is a result of the displacement of O^{2-} and Ti^{4+} from their ideal cubic positions.[1] Other related phases are studied here include $A^{1+}{}_2B^{4+}O_3$ compounds with NaCl-like structures: Na_2ZrO_3, Li_2ZrO_3, Li_2TiO_3, and Li_2SnO_3[5−7]. The oxygen ions show distorted cubic close-packing and the cations occupy the octahedral interstices, thus also forming a cubic close-packed network. It is the way in which the A^{1+} and the B^{4+} atoms are distributed that determines the actual structure. Li_2SnO_3 and Na_2ZrO_3 are isostructural with Li_2TiO_3. Sr_2SnO_4 and Sr_2TiO_4 are examples of a K_2NiF_4-type structure,[8,9] which is built up of perovskite layers of composition $KNiF_3$ and layers of composition KF in the ratio 1:1. By stacking perovskite $SrTiO_3$ with a thickness of more than one layer and SrO layers along the *c*-axis, a range of structures is formed with composition $Sr_{n+1}Ti_nO_{3n+1}$, called Ruddlesden−Popper phases.[8]

Solid state ^{17}O NMR is becoming increasingly established as a tool for characterizing crystalline and amorphous oxide materials in materials chemistry and geochemistry. It is potentially a very attractive nucleus, since it has a wide chemical shift range, making it very sensitive to subtle changes in the atomic scale structure of a material.[10] Additionally it has only

* Address correspondence to this author.
† CSIRO Division of Materials Science and Technology.
‡ University of Kent.
⊗ Abstract published in *Advance ACS Abstracts,* November 1, 1996.

S0022-3654(96)02269-1 CCC: $12.00

a moderate nuclear electric quadrupole moment (eQ). The quadrupole interaction between eQ and the electric field gradient (efg, where eq is the maximum component) broadens the central (1/2, −1/2) transition to second-order[11] which is only partially averaged by magic angle spinning (MAS), contributing to the isotropic shift and complicating spectral interpretation, but the efg can itself provide important structural infomation.[12] This interaction is described by the quadrupole coupling constant $C_Q = e^2qQ/h$. It has been pointed out previously that C_Q for ^{17}O increases as the ionicity of the M−O bond decreases.[13] Oxide perovskites are ionic compounds in which the electrostatic bond strengths (in Pauling's sense) are all smaller than 1; i.e., they are isodesmic.[3] In such highly ionic compounds eq at the oxygen site will be small so that the second-order quadrupolar broadening will be very small, spectral resolution will be high, and correction of the peak position for isotropic quadrupole shifts is unnecessary. The MAS line width provides an upper limit on C_Q which will be less than $(20\nu_L(7.5\Delta)^{1/2}/3)$, where ν_L is the Larmor frequency and Δ is the root mean square line width in ppm.[14] However C_Q cannot then be accurately deduced from the central transition; nevertheless with small interactions the first-order broadened noncentral transitions will produce observable spinning sidebands whose intensity envelope can be used to deduce C_Q.[15] The only drawback of ^{17}O NMR is its low natural abundance (0.037 atom %). Although some natural abundance spectra have been obtained from highly ionic compounds,[14] most work requires isotopic enrichment. It has been shown, that ^{17}O NMR spectra can be readily obtained at an enrichment of only 2.5%.[16,17] ^{17}O NMR has subsequently proved to be very useful in providing insight into the synthesis of many materials including transitional aluminas[18] and sol−gel produced ZrO_2[16] and TiO_2[17], and was able to detect nanoscale phase separation in SiO_2-TiO_2 gels.[19] ^{17}O NMR of perovskites, other than the high temperature superconductors, is somewhat sparse but has been used to examine the local structure and oxide ion motion in defective cubic perovskites such as $Ba(In_{0.67}Zr_{0.33})_yO_{3-y}$.[20]

This paper will present an extensive set of magic angle spinning (MAS) ^{17}O NMR spectra from ABO_3 and A_2BO_3 compounds with A = Li, Na, Ca, Sr, Ba, and La and B = Ti, Zr, Sn, Nb, and Al. As all these structures have an oxygen framework, ^{17}O is the most attractive nucleus to study structural phenomena related to substitution of the various A and B ions within the lattice. The aim is to determine which structural parameters control the ^{17}O NMR chemical shift in perovskites, and also examine if ^{17}O NMR is a good probe of structural distortion. It is shown that the number of resonances in the oxygen spectra and their difference in isotropic chemical shift are very sensitive to deviations of a structure away from cubic symmetry. In addition some multinuclear studies have been carried out on some stannates (^{119}Sn) and comparison is made to a previous study of Clayden et al.[21] Finally the application of ^{17}O and ^{27}Al NMR to following structural development in sol−gel formed $LaAlO_3$ is presented. $LaAlO_3$ is an important material as a possible substrate for high-T_c superconducting films.[22] Above 447 °C $LaAlO_3$ has cubic symmetry, but below 447 °C it adopts a rhombohedrally distorted perovskite structure (space group $R3c$) with the distortion gradually increasing with decreasing temperature.[23,24] $LaAlO_3$ has previously been studied with ^{27}Al and ^{139}La MAS NMR, confirming the presence of single Al and La sites with $\delta_{iso} = 11.7$ ppm, $C_Q = 0.12$ MHz, and $\delta_{iso} = 375 \pm 5$ ppm, $C_Q = 6$ MHz, respectively.[25,26]

Experimental Methods

Li_2CO_3, Sr_2CO_3, and SnO_2 were ^{17}O-enriched by sealing the unenriched compounds with 10 atom % ^{17}O-enriched water in a glass ampule and heating at 110 °C for 2 days. Li_2ZrO_3, $SrZrO_3$, Li_2TiO_3, and $SrTiO_3$ were subsequently prepared by reacting enriched Li_2CO_3 or $SrCO_3$ with ZrO_2 and TiO_2 obtained by hydrolyzing a zirconium or titanium propoxide solution in 2-propanol with ^{17}O-enriched H_2O. Sr_2TiO_4 was obtained by reacting ^{17}O-enriched $SrTiO_3$ and $SrCO_3$ at 900 °C for 24 h. Li_2SnO_3, $SrSnO_3$, and Sr_2SnO_4 were prepared by reaction of stoichiometric amounts of enriched Li_2CO_3 or $SrCO_3$ and SnO_2 at 900−950 °C for 24 h. Heat treatments were performed in platinum crucibles or sintered alumina boats in a dry nitrogen atmosphere. The reaction temperatures of the Sr phases were lowered to 900−950 °C by adding 1 mol of $SrCl_2$ per mol of strontium perovskite as a flux. The zirconates were heated to 600 °C. $CaZrO_3$, $BaZrO_3$, $CaTiO_3$, $BaTiO_3$, and $CaSnO_3$ were obtained by double decomposition of Li_2ZrO_3 or Li_2TiO_3 (Na_2ZrO_3 in case of $CaZrO_3$) with a $BaCl_2$/NaCl or $CaCl_2$/NaCl eutectic mixture at temperatures of 600−850 °C. An X-ray powder pattern of the $CaSnO_3$ sample prepared at 600 °C confirmed it was the low temperature hexagonal form with the ilmenite structure. Subsequent heating to 950 °C converted it into the $GdFeO_3$ structure. A mixture of Nb_2O_5 and Li_2CO_3 was heated with ^{17}O-enriched H_2O at 105 °C in a sealed glass tube for 72 h and subsequent heat treatment at 850 and 950 °C each for 24 h produced $LiNbO_3$. The preparation of Na_2ZrO_3 has been described elsewhere.[27] The identity of all phases was confirmed by X-ray diffraction with a Siemens diffractometer using Ni-filtered Cu Kα radiation.

Isotopically enriched $LaAlO_3$ was prepared by reaction of La_2O_3 with ^{17}O-enriched H_2O in a sealed tube at 130 °C for 72 h, which formed lanthanum hydroxide $La(OH)_3$. The lanthanum hydroxide was then stirred well with an equimolar amount of aluminum propoxide, $Al(OPr)_3$, dissolved in a mixed toluene/2-propanol solvent. Additional ^{17}O-enriched water was added to the stirred suspension. A precipitate formed and the mixture was allowed to stand for 2 weeks while the solvent slowly evaporated in a stream of dry nitrogen at room temperature. The product was heated at successively higher temperatures in dry nitrogen for 2 h periods and examined by X-ray powder diffraction. The mixture of crystalline La_2O_3 and $LaAlO_3$ formed at 950 °C was treated at room temperature with 1 M acetic acid to selectively dissolve lanthanum oxide. After drying, the residue gave an X-ray powder pattern of $LaAlO_3$ with a small admixture of Al_2O_3.

The NMR experiments were carried out on a Bruker MSL 400 spectrometer ($B_0 = 9.4$ T) operating at 54.2, 104.2, and 149.1 MHz for ^{17}O, ^{27}Al, and ^{119}Sn, respectively. For the oxygen MAS spectra, a 7 mm double-bearing (DB) MAS probe was used with 5−6 kHz spinning speeds, 5 s recycle delays and 1.5 μs pulses (flip angle $\sim \pi/4$). Water was used as an external reference ($\delta = 0$ ppm). ^{27}Al NMR spectra were collected using a 4 mm DB MAS probe with spinning speeds of 12 kHz, 0.75 μs pulses, and 1 s recycle delays. The corresponding conditions for ^{119}Sn were 10.5 kHz spinning rates, 2.5 μs pulses and 20 s recycle delays. The ^{27}Al and ^{119}Sn spectra were referenced using the AlO_6 resonance of yttrium aluminum garnet (YAG) at 0.7 ppm and SnO_2 at 0 ppm, respectively (which equals −604.3 ppm relative to the primary tin shift reference tetramethyl tin)[21] as secondary standards.

Results and Discussion

Crystallographic data and the ^{17}O NMR chemical shift and line-width data of the compounds studied are given in Table 1. Typical ^{17}O MAS NMR spectra of a selected group of titanium and zirconium perovskites are displayed in Figure 1. All ^{17}O NMR spectra essentially consist of one or two sharp lines with

TABLE 1: ^{17}O Isotropic Chemical Shifts (δ_{iso}, Relative to H_2O) and Crystallographic Data for ABO_3 and Related Materials

compound	δ_{iso} (ppm)	$\Delta\nu_{MAS}^{(2)}$ (Hz)	C_Q^{max} [a] (MHz)	structure type	space group	no. of O sites	ref for structure
Li_2TiO_3	405.8/372.3	310/310	1.5/1.5	distorted NaCl	*C*2/*c*	3	6
$CaTiO_3$	448.0/443.4	190/n.d.	1.2/n.d.	$GdFeO_3$	*Pbnm*	2	28, 29
$SrTiO_3$	465	240	1.4	perovskite	*Pm*3*m*	1	3
Sr_2TiO_4	426/407	n.d.	n.d.	K_2NiF_4	*I*4/*mmm*	2	8
$BaTiO_3$	564/523[b]	n.d.	n.d.	$BaTiO_3$	*P*4*mm*	2	3, 30
Li_2ZrO_3	298.4/280	350/n.d.	1.6/n.d.	distorted NaCl	*C*2/*c*	2	5
Na_2ZrO_3	308.9/286.0[c]	55/55	0.65	distorted NaCl	*C*2/*c*	3	6
$CaZrO_3$	336/329	n.d.	n.d.	$GdFeO_3$	*Pbnm*	2	28, 29
$SrZrO_3$	343.7/340.2	180/n.d	1.2/n.d.	$GdFeO_3$	*Pbnm*	2	31
$BaZrO_3$	376.0	270	1.4	perovskite	*Pm*3*m*	1	3
Li_2SnO_3	85	2000	3.9	distorted NaCl	*C*2/*c*	3	5
$SrSnO_3$	423	n.d.	3.4	$GdFeO_3$	*Pbnm*	2	32
Sr_2SnO_4	213/198	n.d.	n.d.	K_2NiF_4	*I*4/*mmm*	2	8
$LiNbO_3$	504	1500	3.4	$LiNbO_3$	*R*3*c*	1	33
$LaAlO_3$	170.2	340	1.6		*R*3*c*	1	23

[a] C_Q^{max} are upper estimates for C_Q based on the centerband line width. [b] Data from refs 34 and 35. [c] Data from ref 27.

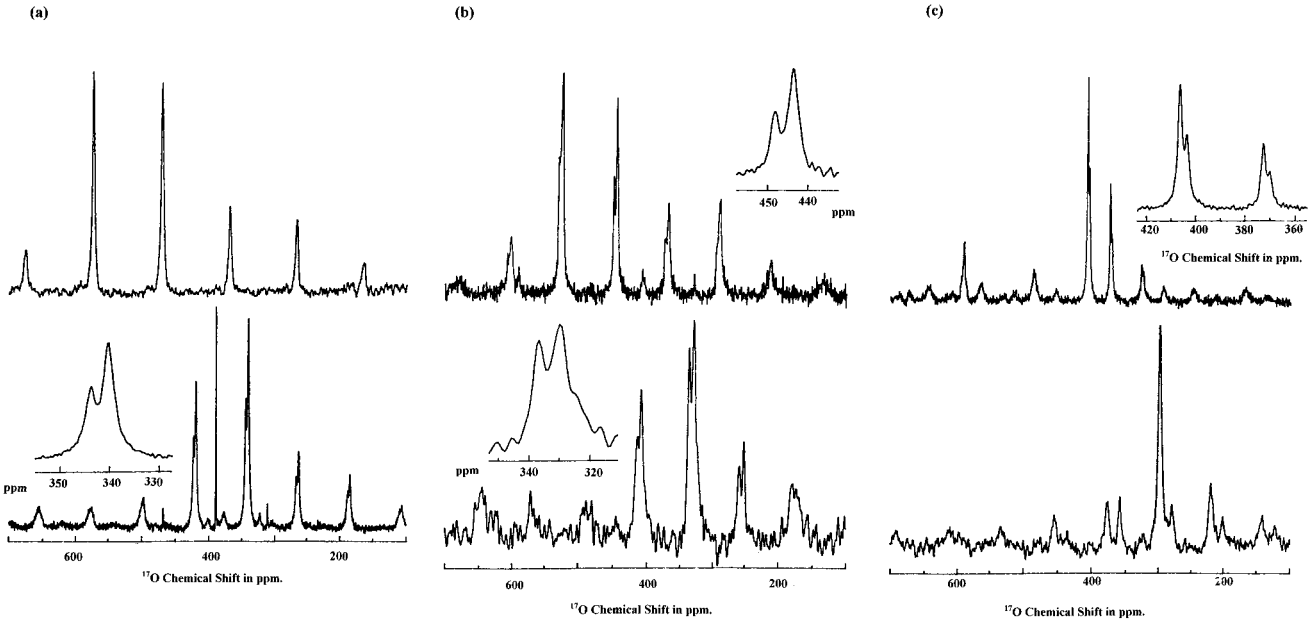

Figure 1. ^{17}O MAS NMR spectra of a selection of titanates (top) and zirconates (bottom) with the same A cation. (a) $SrTiO_3$ and $SrZrO_3$, (b) $CaTiO_3$ and $CaZrO_3$, and (c) Li_2TiO_3 and Li_2ZrO_3. Insets show expansions of the centerbands of the spectra.

their accompanying sidebands. Upper estimates for C_Q derived from the line width are also given in Table 1. As expected from the ionic character of the bonds in these compounds, all values are small; this means that changes in the observed peak position can be largely attributed to chemical changes as there is no significant quadrupole induced contribution.

The most important observation to be made in Figure 1 is that the peak positions of the centerbands of the zirconates are at systematically lower chemical shifts than those of the titanates with the same stoichiometry and A cation. For instance, compare chemical shift data of $BaTiO_3$ (δ_{iso} = 523 and 564 ppm)[34] with that of $BaZrO_3$ (δ_{iso} = 376.0 ppm). Titanates have ^{17}O chemical shifts in the range 372−564 ppm, while zirconates have ^{17}O chemical shifts of 298−376 ppm. This is consistent with earlier results on pure ZrO_2[16] and TiO_2[17] systems. In fact, the ratio between the average ^{17}O chemical shift in isostructural titanates and zirconates with the same A cation is remarkably constant: 0.74 ± 0.03. This value is very close to the ratio of the polarizing powers (α) of Zr^{4+} and Ti^{4+} (where $\alpha = r^2/z$, in which r is the ionic radius (0.64 Å for Ti^{4+} and 0.77 Å for Zr^{4+})[36] and z is the valence of the ion (4 for both ions)). Hence for Ti^{4+} and Zr^{4+} α is 0.41 and 0.59, respectively, so that α_{Ti}/α_{Zr} equals 0.7. This is an indication that in ABO_3 perovskites it is the B ions building up the octahedral network that determine the ^{17}O chemical shift range and not the A ions. The difference in the oxygen NMR data is also reflected in the difference in the Ti−O and Zr−O bond lengths (1.995, and 2.093 Å on average in the compounds in Figure 1) which also reflects the polarizing power.

In addition to the chemical shift differences between the groups with different B cations, there are more subtle effects that influence the actual value of the chemical shift within each group. Most importantly, the number of oxygen resonances increases as the symmetry of the perovskite decreases. $SrTiO_3$ and $BaZrO_3$, both cubic perovskites,[5] have a single sharp ^{17}O resonance as is to be expected since all the oxygen sites are crystallographically equivalent and the sites also have a very small C_Q due to both the site symmetry and ionic nature of the structure. Compounds with the next highest symmetry, $BaTiO_3$ at room temperature and the $GdFeO_3$ type phases, have two ^{17}O signals in the ratio 2:1, also in agreement with their crystallography. In $BaTiO_3$ Ti and Ba are displaced from their ideal positions and the oxygens become inequivalent. In $GdFeO_3$ compounds the BO_6 octahedra are tilted, having the same structural effect.[28,29,31,32] In compounds with an even lower symmetry, the monoclinic *C*2/*c* phases, the number of

oxygen signals does not increase. However the actual ^{17}O chemical shift difference between the resonances increases considerably in the monoclinic $A^{1+}{}_2B^{4+}O_3$ structure. For $GdFeO_3$-structured compounds $CaTiO_3$, $CaZrO_3$, and $SrZrO_3$ the separations are 4.3, 7, and 3.5 ppm, respectively, while for monoclinic Li_2TiO_3, Na_2ZrO_3, and Li_2ZrO_3 the corresponding separations are 33.5, 22.9, and 18.4 ppm, respectively. Dorrian and Newnham[7] refined the Li_2TiO_3 structure and concluded that in $A^{1+}{}_2B^{4+}O_3$ compounds there are only two possible configurations for the oxygen coordination, each with oxygen bonding to two B^{4+} ions and four A^{1+} ions. In the Li_2TiO_3 phases only one of these sites exists, while in Li_2ZrO_3 both configurations are present in a 1:2 ratio. Although in the Li_2TiO_3-type structures only one oxygen geometry is present, the orientation of the OB_2A_4 group within the lattice is different for O(1) and O(3) as compared to O(2). The ^{17}O NMR spectrum of Na_2ZrO_3 has been presented elsewhere[27] and consists of two lines, with an intensity ratio of 1:2, from O(2) and O(1)/O(3) respectively. The oxygen spectrum of Li_2TiO_3 (Figure 1c) is very similar to the Na_2ZrO_3 spectrum, again consisting of two lines in an approximately 2:1 intensity ratio, representing the two distinct oxygen sites, in agreement with the fact that they are isostructural. The only difference between the two spectra is the fact that the two isotropic lines in the Li_2TiO_3 spectrum each consist of a doublet (with approximately equal splittings of 140 Hz). Only two distinct oxygen sites are present in the structure, and the quadrupole interaction is too small to cause quadrupolar structure in the resonances. These compounds are however susceptible to stacking faults, and these effects may be large enough to cause small differences in the chemical shift of 140 Hz.

The ^{17}O NMR spectrum of Li_2ZrO_3 exhibits resonances at 280 and 298.4 ppm in an approximately 1:4 intensity ratio. The Li_2ZrO_3 crystal structure contains two crystallographically distinct oxygen sites O(1) and O(2) in a 1:2 ratio.[5] This discrepancy in intensity has also been observed for Li_2HfO_3, which is isostructural with Li_2ZrO_3.[37] Despite this discrepancy, on the basis of the higher intensity of the 298.4 ppm peak this is attributed to the O(2) site and the 280 ppm resonance to the O(1) site. Li_2SnO_3 is isostructural with Na_2ZrO_3 and Li_2TiO_3, and therefore two resonances would be expected in the ^{17}O NMR spectrum. However, only one broad (fwhh = 1.5 kHz) oxygen signal is observed (Figure 2c). As has been pointed out above, $A^{1+}{}_2B^{4+}O_3$ phases can have a high degree of stacking disorder. Although two-dimensional order exists within the layers of Li and Sn octahedra parallel to the *ab* plane, the double cubic close-packed stacking sequence is absent. As a result, no distinct oxygen resonances are observed, but only one broad signal, which is probably indicative of stacking disorder.

In Sr_2SnO_4 and Sr_2TiO_4, two distinct oxygen sites are present, one within the $SrBO_3$ layer and the other bridging with the Sr. The terminal B−O bonds are shorter (1.90 Å) than the bridging B−O−B (1.94 Å). The oxygen spectra of Sr_2SnO_4 (Figure 2a) and Sr_2TiO_4 (not shown) consist of two lines from the two oxygens in the lattice. The stannate ^{17}O resonances have chemical shifts considerably more shielded than the titanate signals (213/198 ppm and 426/407 ppm, respectively), but the separation is very similar (15 ppm and 19 ppm, respectively). Although the difference in the range of the chemical shifts does not correlate with the difference in the polarizing power, since the ionic radii are almost identical ($r_{Ti^{4+}} = 0.68$ Å, $r_{Sn^{4+}} = 0.71$ Å),[36] it supports the general trend that the most important influence on the chemical shift is the type of B ion; then other smaller effects cause further separation of the resonances. Sr_2SnO_4 and Sr_2TiO_4 are isostructural, and as a result the separation of the constituent resonances is almost identical.

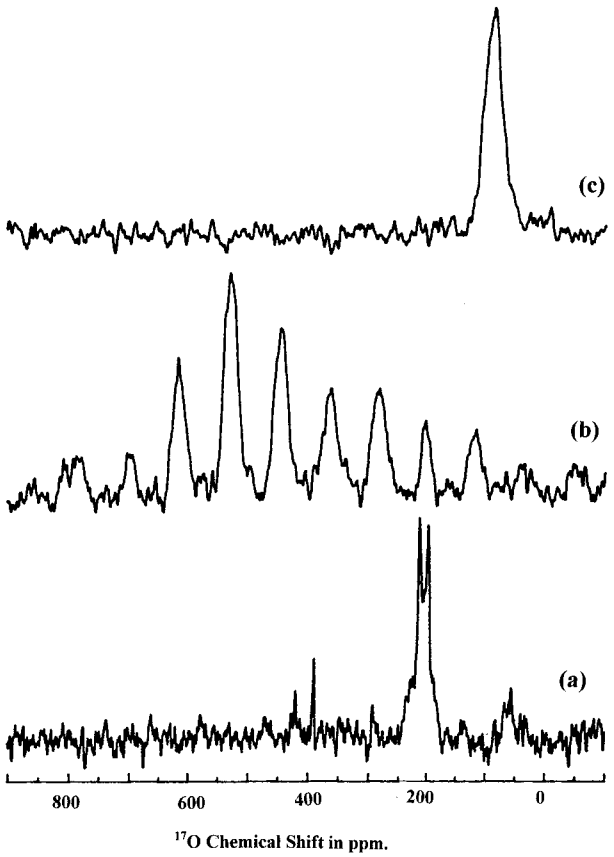

Figure 2. ^{17}O MAS NMR spectra of (a) Sr_2SnO_4, (b) $LiNbO_3$ and (c) Li_2SnO_3.

The ^{17}O NMR spectrum of $BaZrO_3$ is shown in Figure 3. It exhibits a complex spinning sideband envelope that spreads out over a range of approximately 2300 ppm (125 kHz). It is well-known that if the spinning speed under MAS conditions is less than the chemical shift anisotropy, the centerband will be flanked by a series of spinning sidebands,[38] and for spin-1/2 nuclei the intensities of these sidebands can be used to recover the chemical shift parameters.[39] These parameters can be very useful in providing information about the symmetry of the bonding at the nuclear site. For ^{17}O if the quadrupole interaction is not too large ($C_Q \leq 3.3$ MHz), and by applying fast MAS all the transitions are narrowed to form a set of well-defined spinning sidebands. The intensity envelope closely mimics the static line shape and here can be used to accurately determine the quadrupole interaction parameters C_Q and η and the isotropic chemical shift δ_{iso}. Normally the chemical shift anisotropy cannot be directly deduced from such sidebands because of the presence of the quadrupole interaction. The $BaZrO_3$ ^{17}O spectrum represents a special intermediate case of the magnitude of C_Q, in which both the quadrupole interaction and the chemical shift parameters can be effectively estimated independently from different transitions. In the spectrum the two singularities of the ($\pm 3/2$, $\pm 1/2$) transitions are visible, from which $C_Q = 430$ kHz. This value is small and is about one-third of the value of C_Q calculated from the line width (1.4 MHz) emphasizing that ^{17}O residual MAS NMR line widths in many highly ionic crystalline compounds are dominated by chemical shift dispersion, and not by second-order quadrupole effects. Since C_Q is small, it is a very good approximation that the (1/2, −1/2) transition spinning sidebands are determined largely by chemical shift anisotropy (csa). The values for csa derived by Herzfeld and Berger analysis[39] are listed in Table 2. The asymmetry parameter η, expressing the divergence of the chemical shift tensor from axial symmetry, is defined as $(\sigma_{22} - \sigma_{11})/(\sigma_{33} -$

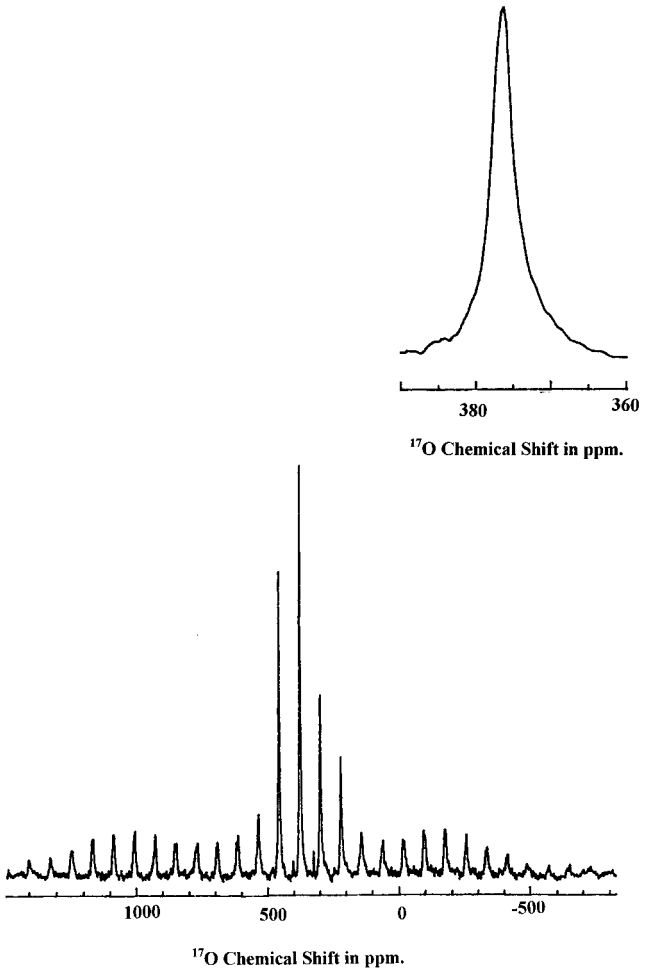

Figure 3. ^{17}O MAS NMR spectrum of $BaZrO_3$. The inset shows an expansion of the centerband.

TABLE 2: NMR Chemical Shift Parameters of a Selected Group of Perovskites

compound	σ_{iso} (ppm)	σ_{11} (ppm)	σ_{22} (ppm)	σ_{33} (ppm)	η	$\Delta\sigma$ (ppm)
$BaZrO_3$	367.2	508	422	171	0.44	−294
$SrTiO_3$	468.1	647	583	174	0.22	−441
$SrZrO_3$	340.1	469	414	137	0.27	−305
$CaTiO_3$	443.9	599	521	211	0.34	−349
$CaZrO_3$	329.3	482	379	126	0.51	−305
$LiNbO_3$	444.7	715	514	105	0.59	−509
$BaTiO_3$[a]	564					−520
	523					−480

[a] Data from ref 34.

σ_{iso}) and ranges between 0 and 1. The divergence from spherical symmetry is expressed by the parameter $\Delta\sigma$ which is defined as $\sigma_{33} - 1/2(\sigma_{22} + \sigma_{11})$.

The most important observation to be made from the values in Table 2 is that the $\Delta\sigma$ values fall in different regions for compounds with different B ions. The values for the titanates are much higher and cover a broader range (−349 to −580 ppm) than the values for the zirconates (−294 to −520 ppm). This is again a reflection of the fact that the B ion is the most important influence on the oxygen chemical shift, being largely responsible for both the magnitude and symmetry of the shielding around the oxygen nucleus.

The $LiNbO_3$ chemical shift interaction derived from sideband analysis (Table 2) does not correspond well with the value anticipated from the shape of the sideband envelope (Figure 2b). A trial Herzfeld and Berger analysis gives 0.6 for the asymmetry parameter, representing a symmetry of the oxygen site which is rather nonaxial. The spectrum, however, indicates that the electron distribution around the oxygen is close to axial (η close to 0, so that $\sigma_{22} - \sigma_{11} \ll \sigma_{33} - \sigma_{iso}$). Herzfeld and Berger analysis is only really applicable to cases where the chemical shift anisotropy is the dominant broadening mechanism of the static spectrum, and the much broader individual lines in this spectrum probably indicate an increase in C_Q (maximum value 3.4 MHz). Compared to the C_Q values of the other compounds studied here (≈400 kHz) $LiNbO_3$ is clearly much higher, and as a result Herzfeld and Berger analysis is not really applicable as the sideband intensity is determined by a convolution of chemical shift and quadrupolar interactions.

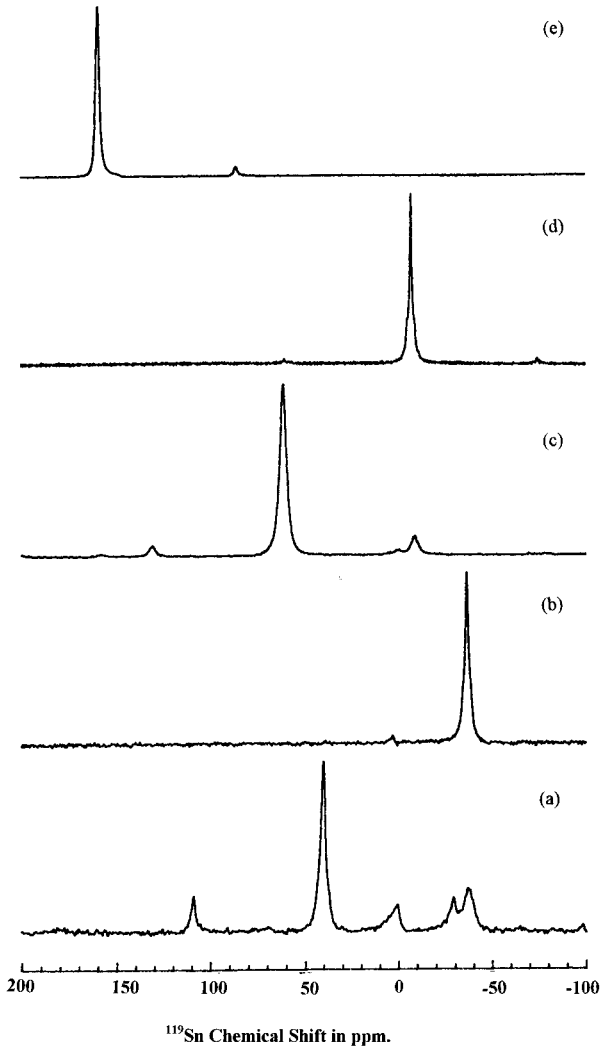

Figure 4. ^{119}Sn MAS NMR spectra of (a) Sr_2SnO_4, (b) $SrSnO_3$, (c) hexagonal $CaSnO_3$, (d) orthorhombic $CaSnO_3$, and (e) Li_2SnO_3. Note the fine structure at the base of the centerbands in (a), (b), and (d), which is interpreted as ^{117}Sn−^{119}Sn spin−spin coupling.

The ^{119}Sn NMR spectra of Sr_2SnO_4, $SrSnO_3$, $CaSnO_3$, and Li_2SnO_3 are displayed in Figure 4. ^{119}Sn shifts for Li_2SnO_3, $SrSnO_3$, Sr_2SnO_4, and the orthorhombic polymorph of $CaSnO_3$ have previously been reported as 160, −36.5, 24.7, and −7.4 ppm, respectively (relative to SnO_2). The Li_2SnO_3 spectrum (Figure 4e) consists of one sharp line at 159.4 ppm. The Sn spectrum of $SrSnO_3$ (Figure 4b) consists of one line with a chemical shift of −36.5 ppm, while the Sr_2SnO_4 spectrum (Figure 4a) has a sharp signal at 40 ppm and broader signals with a low intensity at 0.8 and −37 ppm, representing unreacted SnO_2 and $SrSnO_3$, respectively. Orthorhombic $CaSnO_3$ (Figure 4d) has a shift of −7.4 ppm. The only discrepancy of these results with the data of Clayden et al. is for Sr_2SnO_4 with a

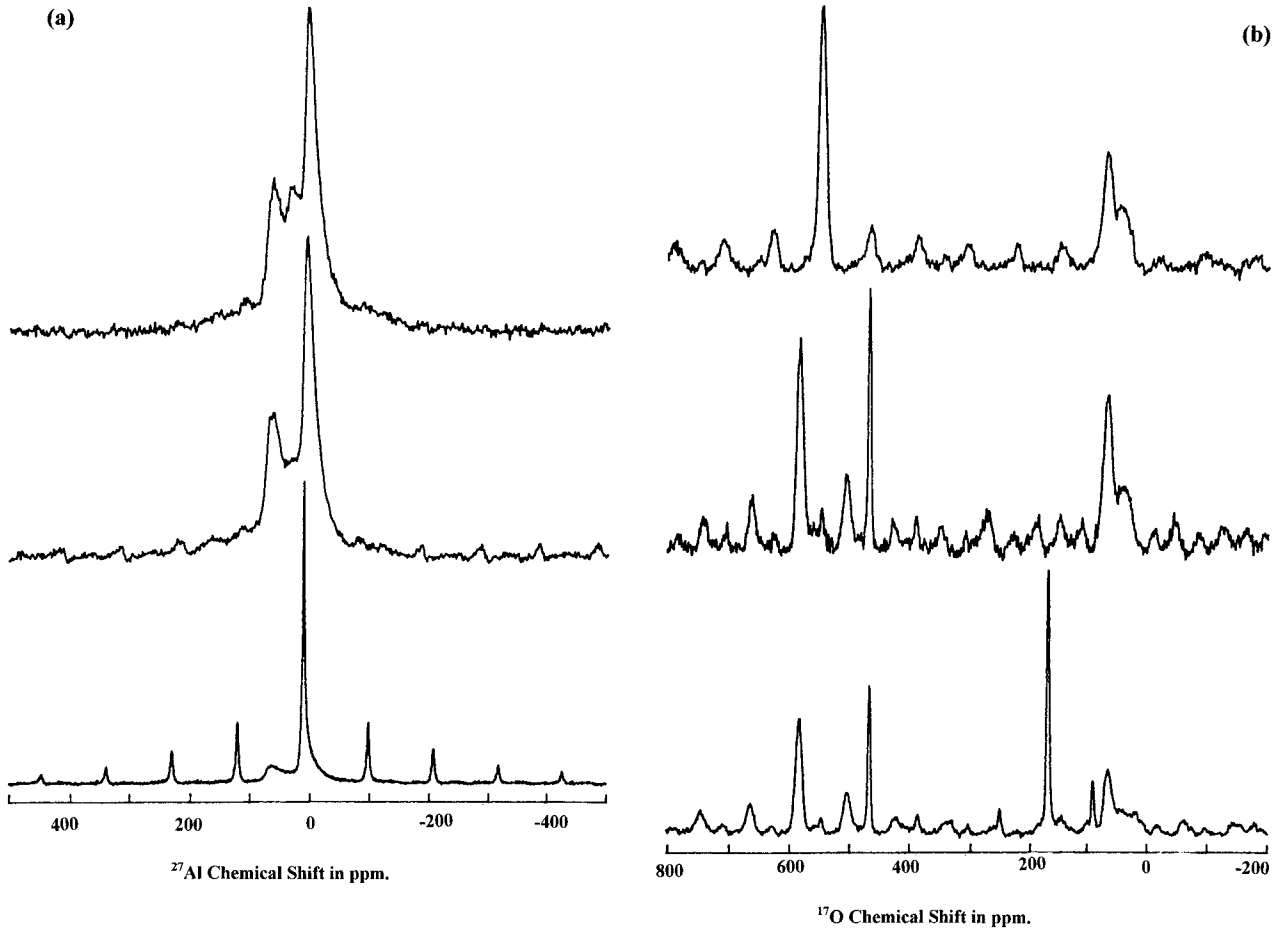

Figure 5. ^{27}Al (a) and ^{17}O (b) MAS NMR spectra of the $LaAlO_3$ mixture at 450 (top), 800, and 950 °C (bottom).

difference of 15.3 ppm. The measurements were repeated here several times, giving consistent results and providing confidence in the values quoted. Close examination of the data of Clayden et al. indicates a difference between the value of the shift presented in their table and the value from their Figure 3, the latter being close to the value obtained here.

$CaSnO_3$ has two polymorphs, a low temperature, hexagonal form and a high temperature, orthorhombic form with a $GdFeO_3$ perovskite structure. Here we report for the first time the ^{119}Sn chemical shift of the hexagonal form of 60.8 ppm (Figure 4c). The data of both $CaSnO_3$ polymorphs show that the structure has a very pronounced effect on the Sn chemical shift, causing a shift difference of 68.2 ppm so that the interesting structure−shift correlation given by Clayden et al. should be limited to isostructural compounds. Close examination of the ^{119}Sn NMR spectra of Sr_2SnO_4, $SrSnO_3$, and $CaSnO_3$ (orthorhombic form) reveals fine structure in the centerbands, which can be attributed to ^{119}Sn−^{117}Sn spin−spin (J) coupling. The magnitude of this interaction varies, but is in the range of 200−300 Hz.

Sol−gel formation of $LaAlO_3$ was examined by X-ray diffraction, ^{27}Al MAS NMR, and ^{17}O MAS NMR. These compounds are all essentially X-ray amorphous except at 950 °C where crystalline La_2O_3 and $LaAlO_3$ have formed so that NMR is necessary to reveal structural information in the intermediate stages. The ^{27}Al MAS NMR spectra of the $LaAlO_3$ mixture at 450, 800, and 950 °C are shown in Figure 5a. At 450 °C the spectrum consists of three broad lines at ≈6.5, 40, and 65 ppm from AlO_4, AlO_5, and AlO_6 sites. The line widths of the lines at 450 and 800 °C indicate that the material is disordered on an atomic scale and the spectra resemble ^{27}Al NMR spectra of amorphous aluminas.[40] The ^{27}Al NMR spectra indicate that the aluminum propoxide has been hydrolyzed and converted into an amorphous aluminum (oxy)hydroxide which has been dehydroxylated with heat treatment. The fraction of AlO_5 decreases with temperature, in agreement with previous studies on amorphous aluminas. At 450 and 800 °C there is no indication in the Al NMR spectra of the form of the lanthanum within the sample. It is only at 950°C that La can be shown to have reacted with the Al component, as the broad AlO_4, AlO_5, and AlO_6 resonances have been converted into one sharp line with a chemical shift of $LaAlO_3$ (11.3 ppm). The marked decrease in the line width indicates an increase in the crystallinity of the sample. The upper limit of the C_Q (1.6 MHz) as determined from the line width (Table 1) corresponds well with the rest of the perovskite phases determined here.

In contrast to the ^{27}Al NMR spectra, the ^{17}O NMR spectra (Figure 5b) contain information on both the La and Al components of the sample at all stages of $LaAlO_3$ synthesis. The spectrum at 450 °C consists of three signals, at 546.4, 68.2, and 44.5 ppm. The two rather broad lines at 68.2 and 44.5 ppm are from oxygens in OAl_4 and OAl_2H units in aluminum (oxy)hydroxides.[18] The signal at 546.4 ppm has been observed before in the synthesis of La_2O_3 using lanthanum propoxide ($La(OPr)_3$) and can be assigned to oxygen in LaOOH.[41] The presence of these different units in the oxygen NMR spectrum indicates that, in the initial gel and in the sample at 450 °C, the La and Al precursors are not atomically mixed and no reaction between them has taken place. At 800 °C, the OAl_4 and OAl_2H units are still present, but the LaOOH unit has been replaced by two signals at 582.4 and 466.5 ppm that can be attributed to oxygens in La_2O_3.[41] Even at this temperature, the La and Al components have not reacted. At 950 °C a new signal at 170.2 ppm appears in the ^{17}O spectrum, while the signals representing the Al and La units have both decreased considerably in

intensity. At this temperature X-ray diffraction indicates the presence of La_2O_3 and $LaAlO_3$ in a 1:1 ratio, and therefore, the 170.2 ppm signal is attributed to $LaAlO_3$. Summarizing, at temperatures <950 °C ^{27}Al NMR only gives information on the Al component of the system, and indicates that Al is present in AlO_4, AlO_5, and AlO_6 coordinations. At 950 °C $LaAlO_3$ has formed. The ^{17}O NMR gives information on both the La and Al components and indicates that at 450 °C these elements are present *separately* as (oxy)hydroxides, which at higher temperatures slowly convert (partly) to oxides and eventually (at a temperature between 800 and 950 °C) react to form $LaAlO_3$.

Conclusion

^{17}O MAS NMR has been shown to be an effective method for probing the structure of mixed metal oxides, and in these highly ionic compounds oxides the line widths are usually small and therefore well-resolved spectra can be obtained. The results show that the ^{17}O chemical shift interaction is dominated by the type of cation building up the octahedral framework (B) and that the cations within the cavities in the structure (A) are of secondary importance. Furthermore, small deviations from the ideal cubic symmetry and the presence of stacking disorder can be readily detected. Application of ^{17}O NMR to the formation of $LaAlO_3$ from aluminum and lanthanum alkoxides clearly provides more insight into the reaction than ^{27}Al NMR and allows structural evolution to be followed. ^{17}O solid state NMR should be increasingly used to characterize ceramic oxide materials in general and is an important component of a multinuclear approach.

Acknowledgment. The authors thank David Hay (CSIRO, Melbourne) for access to the X-ray diffractometer. M.E.S. and P.J.D. thank the EPSRC for funding ^{17}O NMR characterization of materials through Grant GR/J23938.

References and Notes

(1) West, A. R. *Solid State Chemistry and its Applications*; John Wiley & Sons Ltd.: Chichester, 1984.
(2) Ito, E.; Takahashi, E.; Matsui, Y. *Earth Planet. Sci. Lett.* **1984**, *67*, 238.
(3) Megaw, H. D. *Proc. Phys. Soc.* **1946**, *58*, 133.
(4) Glazer, A. M. *Acta Crystallogr.* **1972**, *B28*, 3384.
(5) Hodeau, J. L.; Marezio, M.; Santoro, A.; Roth, R. S. *J. Solid State Chem.* **1982**, *45*, 170.
(6) Dittrich, G.; Hoppe, R. *Z. Anorg. Allg. Chem.* **1969**, *371*, 306.
(7) Dorrian, J. F.; Newnham, R. E. *Mater. Res. Bull.* **1969**, *4*, 179.
(8) Ruddlesden, S. N.; Popper, P. *Acta Crystallogr.* **1957**, *10*, 538.
(9) Weiss, R.; Fairre, R. *C. R. Acad. Sci. Paris* **1959**, *248*, 106.
(10) Oldfield, E.; Coretsopoulos, C.; Yang, S.; Reven, L.; Lee, H. C.; Shore, J.; Han, O. H.; Ramli, E.; Hinks, D. *Phys. Rev. B* **1989**, *40*, 6852.
(11) Cohen, M. H.; Reif, F. *Solid State Phys.* **1957**, *5*, 321
(12) Smith, M. E. *Appl. Magn. Reson.* **1993**, *4*, 1.
(13) Schramm, S.; Oldfield, E. *J. Am. Chem. Soc.* **1984**, *106*, 2502.
(14) Bastow, T. J.; Stuart, S. N. *Chem. Phys.* **1990**, *143*, 459.
(15) Jaeger, C. In *NMR Basic Principles and Progress*; Blumich, B., Kosfeld, R. T., Eds.; Springer-Verlag: Berlin, 1994; Vol. 31, p 134.
(16) Bastow, T. J.; Smith, M. E.; Whitfield, H. J. *J. Mater. Chem.* **1992**, *2*, 989.
(17) Bastow, T. J.; Moodie, A. F., Smith, M. E.; Whitfield, H. J. *J. Mater. Chem.* **1993**, *3*, 697.
(18) Walter, T. H.; Oldfield, E. *J. Phys. Chem.* **1989**, *93*, 6744.
(19) Dirken, P. J.; Smith, M. E.; Whitfield, H. J. *J. Phys. Chem.* **1995**, *99*, 395.
(20) Adler, S.; Russek, S.; Reimer, J.; Fendorf, M.; Stacy, A.; Huang, Q.; Santoro, A.; Lynn, J.; Baltisberger, J.; Werner, U. *Solid State Ionics* **1994**, *68*, 193.
(21) Clayden, N. J.; Dobson, C. M.; Fern, A. *J. Chem. Soc., Dalton Trans.* **1989**, 843.
(22) Guo, R.; Ravindranathan, P.; Selvaraj, U.; Bhalla, A. S.; Cross, L. E.; Roy, R. *J. Mater. Sci.* **1994**, *29*, 5054.
(23) Geller, S.; Bala, V. B. *Acta Crystallogr.* **1956**, *9*, 1019.
(24) Derighetti, B.; Drumheller, J. E.; Lares, F.; Mueller, K. A.; Waldner, F. *Acta Crystallogr.* **1965**, *18*, 557.
(25) Dupree, R.; Lewis, M. H.; Smith, M. E. *J. Am. Chem. Soc.* **1989**, *111*, 5125.
(26) Mueller, K. A.; Brun, E.; Derighetti, B.; Drumheller, J. E.; Waldner, F. *Phys. Lett.* **1964**, *9*, 223.
(27) Bastow, T. J.; Hobday, M. E.; Smith, M. E.; Whitfield, H. J. *Solid State NMR* **1994**, *3*, 49.
(28) Sasaki, S.; Prewitt, C. T.; Liebermann, R. C. *Am. Mineral.* **1983**, *68*, 1189.
(29) Koopmans, H. J.; van de Velde, G. M. H.; Gellings, P. J. *Acta Crystallogr.* **1983**, *C39*, 1323.
(30) Harada, J.; Pedersen, T.; Barnea, Z. *Acta Crystallogr.* **1970**, *A26*, 336.
(31) Ahtee, A.; Ahtee, M.; Glazer, A. M.; Hewat, A. W. *Acta Crystallogr.* **1976**, *B32*, 3243.
(32) Vegas, A.; Vallet-Regí, M.; González-Calbet, J. M.; Alario-Franco, M. A. *Acta Crystallogr.* **1986**, *B42*, 167.
(33) Abrahams, S. C.; Reddy, J. M.; Bernstein, J. L. *J. Phys. Chem. Solids* **1966**, *27*, 997.
(34) Anuradha, V. Masters Thesis, University of Warwick, UK, 1990.
(35) Spearing, D. R.; Stebbins, J. F. *J. Am. Ceram. Soc.* **1994**, *77*, 3263.
(36) Shannon, R. D.; Prewitt, C. T. *Acta Crystallogr.* **1969**, *B25*, 925.
(37) Smith, M. E.; Whitfield, H. J. Unpublished results.
(38) Maricq, M. M.; Waugh, J. S. *J. Chem. Phys.* **1979**, *70*, 3300.
(39) Herzfeld, J.; Berger, A. E. *J. Chem. Phys.* **1980**, *73*, 6021.
(40) Bastow, T. J.; Hall, J. S.; Smith, M. E. *NATO ARW Flash Reaction Processes*; Davis, T. W., Ed.; Kluwer Academic Publishers: Dordrecht, 1995; p 123.
(41) Ali, F.; Smith, M. E.; Steuernagel, S.; Whitfield, H. J. *J. Mater. Chem.* **1996**, *6*, 261.

JP9622694